HHS Public Access

Author manuscript

J Orthop Res. Author manuscript; available in PMC 2017 July 01.

Published in final edited form as:

J Orthop Res. 2016 July ; 34(7): 1111–1120. doi:10.1002/jor.23127.

Multi-Parametric MRI Characterization of Enzymatically Degraded Articular Cartilage

Mikko J. Nissi MJ[*,1,2,3,4,5], **Elli-Noora Salo**[3,6], **Virpi Tiitu**[7], **Timo Liimatainen**[5,8], **Shalom Michaeli**[4], **Silvia Mangia**[4], **Jutta Ellermann**[4], and **Miika T. Nieminen**[2,3,6]

[1]Department of Applied Physics, University of Eastern Finland, Kuopio, Finland [2]Research Unit of Medical Imaging, Physics and Technology, University of Oulu, Oulu, Finland [3]Medical Research Center Oulu, Oulu University Hospital and University of Oulu, Oulu, Finland [4]CMRR, Department of Radiology, University of Minnesota, Minneapolis, MN, USA [5]Diagnostic Imaging Center, Kuopio University Hospital, Kuopio, Finland [6]Department of Diagnostic Radiology, Oulu University Hospital, Oulu, Finland [7]Institute of Biomedicine, Anatomy, University of Eastern Finland, Kuopio, Finland [8]Department of Biotechnology and Molecular Medicine, A. I. Virtanen Institute, University of Eastern Finland, Kuopio, Finland

Abstract

Several laboratory and rotating frame quantitative MRI parameters were evaluated and compared for detection of changes in articular cartilage following selective enzymatic digestion. Bovine osteochondral specimens were subjected to 44h incubation in control medium or in collagenase or chondroitinase ABC to induce superficial collagen or proteoglycan (glycosaminoglycan) alterations. The samples were scanned at 9.4T for T_1, T_{1Gd} (dGEMRIC), T_2, adiabatic $T_{1\rho}$, adiabatic $T_{2\rho}$, continuous-wave $T_{1\rho}$, T_{RAFF2} and T_{1sat} relaxation times and for magnetization transfer ratio (MTR). For reference, glycosaminoglycan content, collagen fibril orientation and biomechanical properties were determined. Changes primarily in the superficial cartilage were noted after enzymatic degradation. Most of the studied parameters were sensitive to the destruction of collagen network, whereas glycosaminoglycan depletion was detected only by native T_1 and T_{1Gd} relaxation time constants throughout the tissue and by MTR superficially. T_1, adiabatic $T_{1\rho}$, adiabatic $T_{2\rho}$, continuous-wave $T_{1\rho}$, and T_{1sat} correlated significantly with the biomechanical properties while T_{1Gd} correlated with glycosaminoglycan staining. The findings indicated that most of the studied MRI parameters were sensitive to both glycosaminoglycan content and collagen network integrity, with changes due to enzymatic treatment detected primarily in the superficial tissue. Strong correlation of T_1, adiabatic $T_{1\rho}$, adiabatic $T_{2\rho}$, continuous-wave $T_{1\rho}$ and T_{1sat} with the altered biomechanical properties, reflects that these parameters were sensitive to critical functional properties of cartilage.

Corresponding author: Mikko J. Nissi, Department of Applied Physics, University of Eastern Finland, POB 1627, FI-70211 Kuopio, Finland, Telephone number: +358-50-5955517, Fax number: +358-17-162585 mikko.nissi@uef.fi.

Author Contribution: Conception and design: MJN, E-NS, MTN. Collection and assembly of data: E-NS, MJN, VT. Analysis of the data: E-NS, MJN, VT. Interpretation of the data: MJN, E-NS, VT, TL, SMa, SMi, JE, MTN. Drafting of the article: MJN, E-NS. Critical revision of the article for important intellectual content: MJN, E-NS, VT, TL, SMa, SMi, JE, MTN. Final approval of the article: MJN, E-NS, VT, TL, SMa, SMi, JE, MTN. Statistical expertise: MJN, E-NS, MTN. Obtaining of funding: MTN.

Keywords

cartilage; MRI; rotating frame of reference; relaxation; biomechanics

Introduction

In addition to direct visualization of cartilage, magnetic resonance imaging (MRI) offers the possibility to probe the interaction between the constituent macromolecules, e.g. collagen, glycosaminoglycans (GAGs) and interstitial water, thus revealing more comprehensive information of the tissue and its status. Several quantitative MRI techniques have been evaluated for the assessment of cartilage properties, including T_2 relaxation time mapping[1-3], native T1 relaxation time mapping[4-6], delayed gadolinium-enhanced MRI of cartilage (the dGEMRIC-technique)[7; 8], $T_{1\rho}$ relaxation time mapping using continuous-wave radio frequency (RF) irradiation (CW-$T_{1\rho}$)[9; 10], magnetization transfer (MT)[11], sodium MRI[12] and chemical exchange saturation transfer (CEST)[13; 14]. Among these techniques, T_2 relaxation time mapping and MT have been mainly linked to the collagen-associated water protons and the integrity of the collagenous matrix, whereas dGEMRIC, sodium MRI and CEST probe the interactions between GAGs and interstitial water either directly or indirectly by using a (negatively) charged contrast agent that distributes into cartilage in inverse proportion to cartilage fixed (negative) charge density. Continuous wave (CW) $T_{1\rho}$ relaxation time has been primarily associated with the GAG content of articular cartilage[9; 10], although association with the properties of the collagen network have also been reported[15].

Recently, an array of novel methods for probing the interactions between tissue macromolecules and water has been introduced[16-18]. Adiabatic rotating frame relaxation methods measure the longitudinal and transverse relaxation times ($T_{1\rho}$ and $T_{2\rho}$) in the rotating frame of reference during adiabatic rotation[19; 20]. In these techniques, a train of adiabatic full-passage (AFP) pulses is applied, creating a time-varying effective magnetic field $B_{\text{eff}}(t)$ which sensitizes the relaxation to a specific frequency range of molecular motion[16; 19]. A further extension of rotating-frame techniques, relaxation along a fictitious field (RAFF), utilizes relaxation during non-adiabatic radio frequency swept pulses[21-23]. With RAFF, the adiabatic condition is violated purposely, allowing substantial reduction of specific absorption rate (SAR) for rotating frame acquisitions. Aside from the rotating-frame methods, a modification to traditional MT method was recently proposed[24]: inclusion of an inversion preparation pulse prior to off-resonance irradiation, which allows markedly larger dynamic range for signal evolution. These novel techniques have been successfully applied to study brain tissue in both animal models[22; 25; 26] and humans[24; 27], and the first results on the application of these techniques to study cartilage degeneration have been promising[16-18].

The aim of this study was to compare an array of both established laboratory frame and less-investigated rotating frame MR parameters in enzymatic collagen and GAG degradation models of articular cartilage. The measured MRI parameters included native T_1 and T_2 relaxation times in the laboratory frame, contrast-enhanced T_1 (i.e. the dGEMRIC index, $T_{1\text{Gd}}$), relaxation time constants in the rotating frame as measured either with continuous-

wave irradiation (CW-$T_{1\rho}$) or with adiabatic techniques (adiabatic $T_{1\rho}$ and $T_{2\rho}$), T_1 relaxation in the presence of off-resonance RF irradiation (T_{1sat}) and magnetization transfer ratio (MTR). The MRI methods were correlated with quantitative microscopy techniques (polarized light microscopy (PLM) of the collagen fibrils and digital densitometry (DD) of Safranin-O stained GAGs), as well as biochemical reference techniques. Finally, the relationship between the MR parameters and mechanical properties of articular cartilage was investigated.

Methods

Sample preparation

Osteochondral cylinders (d = 25 mm, N = 6) were drilled from the lateroproximal facets of intact bovine patellae (N = 6) and cut to three sectors for different treatments (Figure 1). Two of the sectors were enzymatically digested, one using 30 U/ml collagenase (Collagenase type VII (C0773, Sigma-Aldrich Co., St. Louis, MO, USA) and the other using 0.1 U/ml chondroitinase ABC (Seikagaku Co., Tokyo, Japan) to induce primarily collagen degradation or GAG depletion, respectively. The third sector (control) was immersed in Dulbecco's Modified Eagle's Medium (DMEM). All sectors were incubated at +37 °C for 44 hours, cartilage specimens immersed in test tubes surfaces up, without agitation. At 44 hours, to stop the digestion, the specimens were rinsed with and immersed in fresh PBS containing enzyme inhibitors (5 mM EDTA (VWR International LLC, West Chester, PA, USA) and 5 mM Benzamidine HCl5 mM (Sigma-Aldrich)), placed in refrigerator for 2 hours and subsequently frozen at -20 °C for storage before imaging and testing (Figure 1)[2; 28]. Before the biomechanical testing and MRI, each sample was thawed at room temperature.

Biomechanical measurements

Prior to mechanical testing, the thickness of cartilage was determined using 40 MHz ultrasound probe. Cartilage stiffness in the form of equilibrium modulus was determined using stepwise indentation stress-relaxation tests. The sample was mounted on a rigid holder and then compressed using a flat cylindrical indenter of 1 mm diameter in four steps (each step 5% of uncompressed cartilage thickness) up to a strain of 20%[29; 30]. The indentation site was located at the center of each sector. The equilibrium moduli were calculated as described in[2]. After the testing, a smaller osteochondral cylinder (d = 7.2 mm) centered on the mechanical testing location was drilled from each sector for MRI measurements (Figure 1). After preparation, the cylinder was let relax in PBS for 2 hours before MRI. The remaining cartilage tissue was used for biochemical analyses.

MRI

MR experiments were carried out at 9.4 T (Oxford instruments Plc, Witney, UK) with a 19-mm quadrature volume RF transceiver (RAPID Biomedical GmbH, Rimpar, Germany) and Varian VnmrJ 3.1A console (Varian Inc. Palo Alto, CA, USA). The samples were mounted on a custom-made sample holder with cartilage surface oriented perpendicular to the main magnetic field and immersed in perfluoroether (Galden, Solvay, TX, USA). The MR experiments consisted of a preparation block followed by a fast spin echo (FSE) readout

(ETL = 4, TR = 5 s, effective TE = 5 ms, slice thickness 1 mm, matrix size = 256×128 and FOV = 16 × 16 mm^2, yielding a resolution of 62.5 μm along the cartilage depth). The preparation block was modified as presented in Table 1 to measure 8 different MR parameters: native T_1 and T_2 relaxation times, continuous-wave $T_{1\rho}$ relaxation time in the rotating frame (CW-$T_{1\rho}$)[31], adiabatic $T_{1\rho}$ and $T_{2\rho}$ relaxation times in the rotating frame (adiabatic $T_{1\rho}$ and $T_{2\rho}$)[20], relaxation along a fictitious field with rank=2 characterized by time constant T_{RAFF2}[23], longitudinal relaxation time in the presence of RF saturation (T_{1sat})[24] and magnetization transfer ratio (MTR). Following the initial measurements, the samples were rinsed with phosphate buffered saline (PBS) and subsequently immersed in a 1 mM solution of Gd-$DTPA^{2-}$ (Bayer Schering Pharma, Berlin, Germany) in PBS for 24 hours. After the immersion, the contrast-enhanced T_1 relaxation time (T_{1Gd}) was measured using the saturation recovery technique presented in Table 1. After the post-contrast measurements, the samples were processed for histology.

Polarized light microscopy (PLM)

Unstained, formalin-fixed paraffin-embedded samples were cut into 5-μm-thick sections. From each sample, three sections were imaged and averaged. PLM measurements were conducted using a Leitz Ortholux BK-2 polarized light microscope (Leitz Messtechnik GmbH, Wetzlar, Germany) equipped with motor-controlled crossed polarizers, a 2.4 x objective, a monochromatic light source (wavelength λ = 594 ± 3 nm) and a peltier-cooled 12-bit CCD camera (Photometrics SenSys, Roper Scientific Inc., Tucson, AZ, USA). To determine the orientation angle of the collagen fibrils, each section was imaged at multiple orientations of the crossed polarizers using the protocol described previously[32].

Digital densitometry (DD)

The GAG distribution of the samples was assessed with the DD of Safranin-O stained histological sections[33]. The technique is based on the use of a cationic dye, which binds stoichiometrically to the GAG molecules. Optical density (OD), which is linearly related to the staining and thus to GAG content, was determined by measuring the absorbance of monochromatic light (wavelength λ = 492 ± 5 nm). From each sample, three sections of 3-μm thickness were imaged, analysed and averaged to obtain the final OD profile.

Biochemical analyses

The bulk water content and uronic acid (UA) content of the samples were determined biochemically. After measuring the wet weights, the samples were lyophilized, and subsequently the dry weights were determined. The dried samples were incubated with 1 mg/ml concentration of papain (Sigma) in 150 mM sodium acetate including 50 mM Cys-HCl (Sigma) and 5 mM EDTA (Merck, Darmstadt, Germany), pH 6.5, for 3 h at 60°C. The samples were boiled for 10 min to inactivate the enzyme. The UA contents of the digests were quantified from the ethanol-precipitated samples[34]. The amount of UA was normalized to the wet weights of the samples to compensate for the variation in the sample sizes.

Data analysis

All data analysis was conducted using MATLAB (versions R2007b and R2012b, Mathworks Inc., Natick, MA, USA). The relaxation time maps were calculated by fitting the data into respective relaxation time equations. For analysis purposes, four 1-mm wide regions of interest (ROIs) were determined from the center of the cartilage sample: tangential, transitional, radial and full-thickness ROIs, consisting of 5 %, 20 %, 75 % and 100 % of the cartilage thickness (exemplified in Fig. 3). The ROIs were selected to approximately correspond to the distinct zones of collagen orientation in intact cartilage[35; 36]. Furthermore, the full-thickness ROIs were averaged to depth-wise profiles and depth-normalized to 25 points using nearest-neighbour interpolation for group comparisons. The differences between either of the treated sample group and the control group were studied using pair-wise Wilcoxon signed ranks test. The relationships between MRI and reference parameters were studied using Pearson's correlation analysis of pooled data.

Results

The enzymatic treatment of the specimens induced changes in their biochemical and biophysical properties. Both enzymes affected primarily the superficial articular cartilage, as can be appreciated in the Safranin-O-stained sections of a representative specimen after chondroitinase ABC, collagenase and control treatments (Figure 2). The mechanical stiffness of the chondroitinase ABC and collagenase treated groups was significantly lower than that of the control specimens (Table 2). The UA content and optical density, both reflective of the glycosaminoglycan content, were significantly lower in the chondroitinase ABC treated group as compared to the controls, while no significant difference was noted for the collagenase treated specimens (Table 2). The bulk water contents were slightly increased in the treated groups, however without statistical significance (Table 2).

The sensitivity of the different quantitative MRI parameters to the enzymatic treatments was variable (Figure 3). As shown in the zoomed inserts of the Safranin-O-stained microscopy sections (Figure 2), the surface of the specimens was changed especially after the collagenase treatment, seen particularly in the T_2, adiabatic $T_{2\rho}$ and T_{RAFF2} maps, whereas a more uniform depletion of GAGs was observed after the chondroitinase ABC treatment (Figure 3). The depth-wise changes in the MRI parameters between the control and treated specimen groups were assessed in the depth-normalized profiles (Figure 4). Both the native T_1 relaxation time and T_1 relaxation time in the presence of Gd-DTPA^{2-} ($T_{1\mathrm{Gd}}$, i.e. dGEMRIC index) detected differences between chondroitinase-treated and control groups at several depths through the cartilage thickness, whereas almost all parameters detected differences limited to the most superficial tissue after the collagenase treatment ($p < 0.05$, Wilcoxon signed ranks test, Figure 4). Optical density, reflective of the GAG content, showed differences between the chondroitinase-treated and control specimens from the cartilage surface to about 30% depth and in the deep part of the tissue, and only in a thin layer at the most superficial tissue between the collagenase-treated and control specimens (Figure 4). On the other hand, the collagen fibril orientation angle, as determined by PLM, demonstrated significant difference between the collagenase-treated and control specimens in the superficial part of the tissue (Figure 4). The standard deviations of the group-average

profiles are not shown in Figure 4, but were fairly large, explaining regions that had large apparent difference without statistical significance (Figure 4).

Several of the different MRI parameters in the four defined ROIs demonstrated significant differences between the control specimens and collagenase treated or chondroitinase ABC treated specimens (Table S-1). For the collagenase treated specimens, differences were primarily noted in the tangential and transitional ROIs, as well as in the full-thickness ROI, indicative of the surface of the specimens primarily affected in the treatment (Table S-1). Except for T_{1Gd} and MTR, which did not show statistically significant differences between the collagenase treated and the control groups, all the relaxation times were increased in the treated specimens (Table S-1). For chondroitinase ABC treated specimens, the pattern was more complicated: native T_1 relaxation time demonstrated statistically significant increase while T_{1Gd} demonstrated significant decrease throughout the tissue thickness; otherwise only MTR in the superficial ROI was significantly different (decreased) (Table S-1). The rest of the relaxation times, except for T_{RAFF2} in the superficial tissue, did not significantly change (Table S-1).

For pooled data (all three groups together), the equilibrium mechanical stiffness correlated significantly with T_1, CW-$T_{1\rho}$, adiabatic $T_{1\rho}$, adiabatic $T_{2\rho}$, and T_{1sat} parameters with correlation coefficients ranging from -0.573 to -0.637, assessed for the bulk cartilage ROI, whereas the rest of the parameters, T_{1Gd}, T_2 and T_{RAFF2} relaxation times and MTR demonstrated no significant correlation with mechanical stiffness (Table 3). Only T_{1Gd} correlated significantly with uronic acid content ($r = 0.699$, $p = 0.001$) and bulk optical density, while CW-$T_{1\rho}$, adiabatic $T_{1\rho}$ and T_{1sat} correlated significantly with the water content (Table 3).

Discussion

The sensitivity of numerous quantitative MRI parameters for enzymatically-induced degradation of bovine articular cartilage was evaluated in the present study. The parameters studied included several that have been under investigation for years, some of which have been implemented in clinical practise (T_2 relaxation time, T_{1Gd} relaxation time, i.e. dGEMRIC technique and CW-$T_{1\rho}$ relaxation time). In addition, several recently introduced or otherwise less studied quantitative MRI parameters were included, such as adiabatic $T_{1\rho}$ and $T_{2\rho}$, T_{RAFF2}, T_{1sat} relaxation times, magnetization transfer ratio and T_1 relaxation time[16-18; 27]. While T_1 relaxation time in the assessment of articular cartilage has been investigated previously, it has received less attention than perhaps warranted[5]. Many of the parameters were found sensitive to the enzymatic degradation and a range of correlations with reference properties was established.

The degeneration models employed, collagenase treatment and chondroitinase ABC treatment are both models that have been commonly used and established for inducing differential and mostly constituent-specific degradation in articular cartilage[2; 37; 38]. Collagenase enzyme primarily targets the collagen fibrils in the cartilage matrix, digesting native collagen in the triple helix region[39; 40], whereas chondroitinase ABC primarily affects the proteoglycans by cleaving the GAG side chains chondroitin and dermatan sulfate, as

well as hyaluronic acid[41; 42]. While collagenase affects mainly the collagen fibril network, it induces degradation and secondary changes in the GAG content as well; after the supporting framework of the collagens is destroyed, GAG loss is also caused[2; 38; 43; 44]. The chosen treatment procedures induced changes in the cartilage matrix reaching to a depth of approximately one third at maximum. The primary changes were limited to the superficial portion of the tissue and as such, can be considered representative of tissue changes typical to relatively mild cartilage degeneration. Although no significant changes in the GAG content of the collagenase-treated specimens was observed, the surface of the specimens appeared visually fibrillated. A previous study demonstrated the sensitivity and robustness of several of the parameters investigated in this study by using a PG depletion model with trypsin[16]. In this study, significantly subtler changes limited primarily to the superficial part of the tissue were induced; despite the increased challenge, many of the investigated parameters were still confirmed to be sensitive to the induced changes.

The reference measurements, especially the mechanical stiffness of the specimens revealed that the tissue properties changed significantly with the treatments. Young's modulus at equilibrium was decreased especially after the chondroitinase ABC treatment, in line with previous publications indicating GAGs as the main determinant of the equilibrium stiffness[38]. The equilibrium stiffness was significantly reduced also after the collagenase treatment, although typically larger changes in the instantaneous stiffness or the fibril network module are observed after collagenase[38]. Furthermore, the changes in the equilibrium stiffness values were in agreement with those previously reported for specimens treated with similar procedures[38]. The bulk GAG content, as indicated by average OD or uronic acid content was significantly reduced in the chondroitinase ABC treated specimens, but not in the collagenase treated. However, the collagenase treatment affected the collagen fibril network in the superficial tissue markedly more than the chondroitinase ABC treatment, as was indicated by the fibril orientation measurement by PLM. In deeper parts of the tissue the fibril orientation as well as the GAG content appeared approximately equal in all groups, further indicating the superficial part of the tissue as the mainly affected region. The histological findings highlight the interdependence of GAG loss and associated collagen network alterations following chondroitinase ABC treatment. This feature is critical, since it has been observed that GAG loss is associated with the early stages of cartilage degeneration[45-47].

Out of the quantitative MRI parameters studied, the most frequently investigated ones, namely T_2, T_{1Gd} and CW-$T_{1\rho}$ relaxation times demonstrated variable and complementary sensitivity to the induced changes, as indicated by the different correlations with the reference parameters (Table 3). T_{1Gd} relaxation time constant was the only parameter that significantly correlated with the uronic acid content and the optical density of Safranin-O-stained sections, both reflective of GAG content, although similar trends were observed also for T_1, $T_{2\rho}$ and both $T_{1\rho}$ relaxation time constants[48]. T_{1Gd} and CW-$T_{1\rho}$ have both been connected to the proteoglycan (glycosaminoglycan) content in cartilage[7; 9; 48]. In the present study, CW-$T_{1\rho}$ showed a small increase with decrease of GAG content, even if without reaching significance; instead, a significant correlation with the mechanical properties was noted, also in line with previously established findings[49]. The spin-lock amplitude in the present study was set to 1 kHz; most of the previous in vivo studies have been conducted at a

spin-lock amplitude of 500 Hz. Lower amplitude (250 Hz and below) increases sensitivity to residual dipolar coupling[50; 51]. Our earlier results on $T_{1\rho}$ dispersion[18] indicated that in ex vivo human cartilage, a range of 250 -1000 Hz spin-lock power is sensitive to changes due to natural degeneration and correlated with measured properties of cartilage. The CW-$T_{1\rho}$ values at 1 kHz spin-lock amplitude were slightly higher than those typically measured in vivo at lower spin-lock amplitude[52], but the observed changes had the same trends. T_2 relaxation time constant is generally considered to be reflective of the properties and integrity of the collagen fibril network[1; 2; 36; 53]. In this study, the T_2 relaxation was also found not to correlate with the GAG content and not to demonstrate significant differences between the control and chondroitinase ABC treated specimens. However, in accordance with the previous publications, a significant difference in all but the radial zone (least affected by the enzymes) was found for T_2 relaxation time constant between the control and collagenase treated groups, indicating the integrity of the collagen fibril network and likely also the sensitivity to the magic angle effect as the main contributors in the changes of T_2. The bulk T_2 values in the present study were comparable with those previously published for in vivo measurements[52]; the larger superficial T_2 values of the treated specimens were consistent with the degradation of the tissue[2].

The novel MRI parameters investigated, namely adiabatic $T_{1\rho}$, adiabatic $T_{2\rho}$, inversion-prepared MT (T_{1sat}) and T_{RAFF2} were found significantly affected by the collagenase treatment except in the deep tissue, whereas the chondroitinase ABC treatment did not induce significant changes in these parameters. With the exception of T_{RAFF2}, the parameters also correlated significantly with the mechanical properties of the tissue specimens and with the exception of T_{RAFF2} and adiabatic $T_{2\rho}$, the parameters also significantly correlated with the bulk water content. The chondroitinase ABC treatment affected both native T_1 and T_{1Gd} significantly throughout the tissue depth, and MTR in the superficial ROI; other investigated parameters were not significantly changed by the treatment. The findings are somewhat in contrast with the significant changes reported for trypsin-digested bovine patellar cartilage specimens not only for adiabatic $T_{1\rho}$, but also for T_{RAFF2}[16]. However, a brief comparison of the Safranin-O-staining in Fig. 2 to the Safranin-O-fast green staining in Fig. 3 of the previous study[16] demonstrates the radically more aggressive GAG depletion in the previous study. This difference showcases the sensitivity of the techniques: even in a very modest digestion model, the parameters either demonstrated a small, though non-significant change, or even a significant difference as was observed for collagenase-treated specimens. In another previous study, comparing human tibial cartilage specimens with naturally occurring mild and advanced osteoarthritis (OA), a significant difference between the two disease stages was observed in all of the aforementioned novel quantitative MRI parameters[18]. Furthermore, in a rabbit anterior cruciate ligament transection OA-model, T_{RAFF2} again did not show significant difference between affected and control knees[17]. Besides differences in the species investigated (bovine vs. rabbit vs. human) or the type of enzymatic degradation, differences in the measurement geometry exist between the present and the previous studies: here, the specimens were oriented cartilage surface normal along the main field, whereas in the previous investigations, the specimens were oriented either at the magic angle[16] or perpendicular to the main field[17]. The orientation dependence of these novel (as well as the established) MRI parameters has been

briefly investigated[51] and found to be a factor affecting the observed relaxation times. Taken together, the novel parameters appear promising in the assessment of articular cartilage, but also exhibit sensitivity to the species origin and type of articular cartilage investigated. Perhaps the only exception is adiabatic $T_{1\rho}$, which uniformly shows sensitivity to degeneration or enzymatic degradation of articular cartilage in this and several previous studies[16-18; 54].

Certainly not a novel parameter, but one, which has been left on limited attention is native T_1 relaxation time constant. In the present study T_1 correlated significantly with the equilibrium mechanical modulus and demonstrated a significant change after the chondroitinase ABC treatment throughout the tissue depth. However, T_1 relaxation time had a very weak correlation with the bulk water content in these enzymatically treated specimens for bovine patella, in contrast to earlier study on non-treated cartilage specimens from different joint surfaces in the bovine knee[4]. T_1 relaxation time constant has been occasionally reported in cartilage MRI investigations and found sensitive to changes in cartilage, often with increased values due to disease or treatment[5; 55; 56], but also with decreased values due to treatment[57] or to correlate with, for example mechanical properties or GAG content[6; 58]. This may be due to the effect of different degrading medium on tissue proteins, hence, differently reflected in relaxation times

As evidenced by the reference methods as well as the depth-wise dependence of the relaxation time and reference parameter plots in Fig. 4, the changes due to the enzymatic treatment were mostly limited to the superficial part of the tissue. This fairly small induced change can be viewed as a limitation of the study as it represents only mild, local degenerative changes of tissue and does not necessarily correspond to all forms of OA. Furthermore, as the changes were predominantly limited to the superficial part of the tissue, sensitivity of the bulk biochemical reference parameters is severely limited, as was reflected by the fairly modest changes detected by the biochemical measurements. However, as it still permits detection of significant differences with various MRI parameters, it provides a model of changes possibly comparable to relatively early changes in OA and is thus relevant despite the modest changes observed. This highlights the importance of spatial analysis of cartilage properties and the importance of spatial reference methods[37]. Another factor potentially affecting the observed differences is that the samples in the different groups were adjacent tissue, and may slightly differ due to natural biological variation. The spatial separation of the cylindrical sample cores was approximately 11 mm center-to-center. Furthermore, the effect of the enzymes is more specific than the effect of OA, thus providing insight into the specificities of the different parameters. The small number of specimens is also an acknowledged limitation of the study, reducing the statistical power; thus a robust non-parametric statistical test was employed. A noted confounding factor in quantitative MRI studies is the solution the specimens are imaged in; significant differences in relaxation times have been reported for different constituent-extracting solutions as compared to normal saline[57]. In the present study, however, the specimens were always rinsed with fresh PBS before imaging, resulting in comparable imaging conditions between the control and treated specimens. For high concentration PBS, a significant effect has also been shown[59]. In this study, however, approximately ten-fold lower phosphate concentration was used. Additionally, the freeze-thaw cycle in the sample processing may have affected the

properties of the samples[60], but was a necessity due to sample logistics. It has been shown that an analysis done immediately after thawing of the cartilage tissue, as was done in this study, should not be significantly affected by leakage of GAGs to the bathing medium[61]. On the other hand, for the dGEMRIC experiment, T_{1Gd} was measured after 24 hours of equilibration in contrast medium, which may have resulted in additional leakage of GAGs. However, the handling protocol was the same for all specimens and except for potentially increased leakage of GAGs from the treated specimens should have similar effects and thus allow comparison between the groups. As noted above, the sensitivity of the MRI parameters to orientation of cartilage in the magnetic field has been demonstrated for several of the studied parameters[1; 51; 62; 63]. The orientation dependence may also be considered as a limitation, as it affects any MRI measurement especially in the *in vivo* situation where the orientation cannot be controlled; in the present study care was taken to orient all the specimens in exactly the same way in the static magnetic field.

In conclusion, multiple quantitative MRI parameters were investigated in this enzymatic treatment model of cartilage degeneration with minor degenerative changes. Differences between the control and either of the treated groups were noted for several of the investigated MRI parameters. Importantly, strong correlations with biomechanical properties of the specimens were observed for adiabatic $T_{1\rho}$, CW-$T_{1\rho}$, T_{1sat} and native T_1, indicating that changes in critical functional properties of cartilage are reflected in the MRI parameters. Perhaps somewhat surprisingly, native T_1 relaxation time was found sensitive to the changes induced by the chondroitinase ABC treatment throughout the tissue depth, suggesting that in the assessment of cartilage, native T_1 deserves more attention than it has typically received. Taking into account the present and recently published findings, adiabatic $T_{1\rho}$ appears sensitive to degenerative changes of cartilage, regardless of the specific type or species origin, and warrants further investigation especially in the clinical setting.

Supplementary Material

Refer to Web version on PubMed Central for supplementary material.

Acknowledgments

This study was supported by the Academy of Finland (grants 128603, 260321, 285909), TBDP National Doctoral Programme of Musculoskeletal Disorders and Biomaterials, Finland, Orion Research Foundation and NIH grant P41 EB015894.

References

1. Xia Y. Relaxation anisotropy in cartilage by NMR microscopy (muMRI) at 14-microm resolution. Magn Reson Med. 1998; 39:941–949. [PubMed: 9621918]
2. Nieminen MT, Töyräs J, Rieppo J, et al. Quantitative MR microscopy of enzymatically degraded articular cartilage. Magn Reson Med. 2000; 43:676–681. [PubMed: 10800032]
3. Nieminen MT, Rieppo J, Töyräs J, et al. T2 relaxation reveals spatial collagen architecture in articular cartilage: a comparative quantitative MRI and polarized light microscopic study. Magn Reson Med. 2001; 46:487–493. [PubMed: 11550240]
4. Berberat JE, Nissi MJ, Jurvelin JS, et al. Assessment of interstitial water content of articular cartilage with T1 relaxation. Magn Reson Imaging. 2009; 27:727–732. [PubMed: 19056195]

5. Lin PC, Reiter DA, Spencer RG. Sensitivity and specificity of univariate MRI analysis of experimentally degraded cartilage. Magn Reson Med. 2009; 62:1311–1318. [PubMed: 19705467]
6. Nissi MJ, Töyräs J, Laasanen MS, et al. Proteoglycan and collagen sensitive MRI evaluation of normal and degenerated articular cartilage. J Orthop Res. 2004; 22:557–564. [PubMed: 15099635]
7. Bashir A, Gray ML, Burstein D. Gd-DTPA^{2-} as a measure of cartilage degradation. Magn Reson Med. 1996; 36:665–673. [PubMed: 8916016]
8. Bashir A, Gray ML, Hartke J, et al. Nondestructive imaging of human cartilage glycosaminoglycan concentration by MRI. Magn Reson Med. 1999; 41:857–865. [PubMed: 10332865]
9. Duvvuri U, Reddy R, Patel SD, et al. T(1r)-relaxation in articular cartilage: effects of enzymatic degradation. Magn Reson Med. 1997; 38:863–867. [PubMed: 9402184]
10. Akella SV, Regatte RR, Gougoutas AJ, et al. Proteoglycan-induced changes in T1r-relaxation of articular cartilage at 4T. Magn Reson Med. 2001; 46:419–423. [PubMed: 11550230]
11. Gray ML, Burstein D, Lesperance LM, et al. Magnetization transfer in cartilage and its constituent macromolecules. Magnetic Resonance in Medicine. 1995; 34:319–325. [PubMed: 7500869]
12. Borthakur A, Mellon E, Niyogi S, et al. Sodium and T1rho MRI for molecular and diagnostic imaging of articular cartilage. NMR Biomed. 2006; 19:781–821. [PubMed: 17075961]
13. Ling W, Regatte RR, Navon G, et al. Assessment of glycosaminoglycan concentration in vivo by chemical exchange-dependent saturation transfer (gagCEST). Proc Natl Acad Sci U S A. 2008; 105:2266–2270. [PubMed: 18268341]
14. Ling W, Regatte RR, Schweitzer ME, et al. Characterization of bovine patellar cartilage by NMR. NMR Biomed. 2008; 21:289–295. [PubMed: 17659534]
15. Mlynárik V, Szomolanyi P, Toffanin R, et al. Transverse relaxation mechanisms in articular cartilage. J Magn Reson. 2004; 169:300–307. [PubMed: 15261626]
16. Ellermann J, Ling W, Nissi MJ, et al. MRI rotating frame relaxation measurements for articular cartilage assessment. Magn Reson Imaging. 2013; 31:1537–1543. [PubMed: 23993794]
17. Rautiainen J, Nissi MJ, Liimatainen T, et al. Adiabatic rotating frame relaxation of MRI reveals early cartilage degeneration in a rabbit model of anterior cruciate ligament transection. Osteoarthritis Cartilage. 2014; 22:1444–1452. [PubMed: 25278055]
18. Rautiainen J, Nissi MJ, Salo EN, et al. Multiparametric MRI assessment of human articular cartilage degeneration: Correlation with quantitative histology and mechanical properties. Magn Reson Med. 2014
19. Michaeli S, Sorce DJ, Garwood M. T-2 rho and T-1 rho adiabatic relaxations and contrasts. Curr Anal Chem. 2008; 4:8–25.
20. Michaeli S, Sorce DJ, Idiyatullin D, et al. Transverse relaxation in the rotating frame induced by chemical exchange. J Magn Reson. 2004; 169:293–299. [PubMed: 15261625]
21. Liimatainen T, Hakkarainen H, Mangia S, et al. MRI contrasts in high rank rotating frames. Magn Reson Med. 2014
22. Liimatainen T, Mangia S, Ling W, et al. Relaxation dispersion in MRI induced by fictitious magnetic fields. J Magn Reson. 2011; 209:269–276. [PubMed: 21334231]
23. Liimatainen T, Sorce DJ, O'Connell R, et al. MRI contrast from relaxation along a fictitious field (RAFF). Magn Reson Med. 2010; 64:983–994. [PubMed: 20740665]
24. Mangia S, De Martino F, Liimatainen T, et al. Magnetization transfer using inversion recovery during off-resonance irradiation. Magn Reson Imaging. 2011; 29:1346–1350. [PubMed: 21601405]
25. Liimatainen T, Sierra A, Hanson T, et al. Glioma cell density in a rat gene therapy model gauged by water relaxation rate along a fictitious magnetic field. Magn Reson Med. 2012; 67:269–277. [PubMed: 21721037]
26. Jokivarsi KT, Niskanen JP, Michaeli S, et al. Quantitative assessment of water pools by T 1 rho and T 2 rho MRI in acute cerebral ischemia of the rat. Journal of cerebral blood flow and metabolism : official journal of the International Society of Cerebral Blood Flow and Metabolism. 2009; 29:206–216.

27. Liimatainen, T.; Nissi, MJ.; Nieminen, MT., et al. Proc Intl Soc Mag Reson Med. Stockholm, Sweden: 2010. Relaxation along Fictitious Field (RAFF) Contrast in Bovine Articular Cartilage; p. 836
28. Laasanen MS, Töyräs J, Hirvonen J, et al. Novel mechano-acoustic technique and instrument for diagnosis of cartilage degeneration. Physiol Meas. 2002; 23:491–503. [PubMed: 12214758]
29. Korhonen RK, Laasanen MS, Töyräs J, et al. Comparison of the equilibrium response of articular cartilage in unconfined compression, confined compression and indentation. J Biomech. 2002; 35:903–909. [PubMed: 12052392]
30. Töyräs J, Laasanen MS, Saarakkala S, et al. Speed of sound in normal and degenerated bovine articular cartilage. Ultrasound Med Biol. 2003; 29:447–454. [PubMed: 12706196]
31. Grohn OH, Makela HI, Lukkarinen JA, et al. On- and off-resonance T(1rho) MRI in acute cerebral ischemia of the rat. Magn Reson Med. 2003; 49:172–176. [PubMed: 12509834]
32. Rieppo J, Hallikainen J, Jurvelin JS, et al. Practical considerations in the use of polarized light microscopy in the analysis of the collagen network in articular cartilage. Microsc Res Tech. 2008; 71:279–287. [PubMed: 18072283]
33. Király K, Lammi M, Arokoski J, et al. Safranin O reduces loss of glycosaminoglycans from bovine articular cartilage during histological specimen preparation. Histochem J. 1996; 28:99–107. [PubMed: 8737291]
34. Blumenkrantz N, Asboe-Hansen G. New method for quantitative determination of uronic acids. Anal Biochem. 1973; 54:484–489. [PubMed: 4269305]
35. Xia Y. Heterogeneity of cartilage laminae in MR imaging. J Magn Reson Imaging. 2000; 11:686–693. [PubMed: 10862069]
36. Nissi MJ, Rieppo J, Töyräs J, et al. T(2) relaxation time mapping reveals age- and species-related diversity of collagen network architecture in articular cartilage. Osteoarthritis Cartilage. 2006; 14:1265–1271. [PubMed: 16843689]
37. Griffin DJ, Vicari J, Buckley MR, et al. Effects of enzymatic treatments on the depth-dependent viscoelastic shear properties of articular cartilage. J Orthop Res. 2014; 32:1652–1657. [PubMed: 25196502]
38. Korhonen RK, Laasanen MS, Töyräs J, et al. Fibril reinforced poroelastic model predicts specifically mechanical behavior of normal, proteoglycan depleted and collagen degraded articular cartilage. J Biomech. 2003; 36:1373–1379. [PubMed: 12893046]
39. Harris ED Jr, Parker HG, Radin EL, et al. Effects of proteolytic enzymes on structural and mechanical properties of cartilage. Arthritis Rheum. 1972; 15:497–503. [PubMed: 4343998]
40. Shingleton WD, Hodges DJ, Brick P, et al. Collagenase: a key enzyme in collagen turnover. Biochem Cell Biol. 1996; 74:759–775. [PubMed: 9164646]
41. Derby MA, Pintar JE. The histochemical specificity of Streptomyces hyaluronidase and chondroitinase ABC. Histochem J. 1978; 10:529–547. [PubMed: 80394]
42. Murata K, Bjelle AO. Constitutional heterogeneity of the glycosaminoglycans in articular cartilage proteoglycans. Connect Tissue Res. 1977; 5:109–116. [PubMed: 142604]
43. Kempson GE, Tuke MA, Dingle JT, et al. The effects of proteolytic enzymes on the mechanical properties of adult human articular cartilage. Biochim Biophys Acta. 1976; 428:741–760. [PubMed: 1276179]
44. Rieppo J, Töyräs J, Nieminen MT, et al. Structure-function relationships in enzymatically modified articular cartilage. Cells Tissues Organs. 2003; 175:121–132. [PubMed: 14663155]
45. Buckwalter JA, Mankin HJ. Articular Cartilage, Part II: Degeneration and osteoarthrosis, repair, regeneration, and transplantation. J Bone Joint Surg Am. 1997; 79:612–632.
46. Mankin HJ, Dorfman H, Lippiello L, et al. Biochemical and metabolic abnormalities in articular cartilage from osteo-arthritic human hips. II. Correlation of morphology with biochemical and metabolic data. J Bone Joint Surg Am. 1971; 53:523–537. [PubMed: 5580011]
47. Lohmander LS. Articular cartilage and osteoarthrosis. The role of molecular markers to monitor breakdown, repair and disease. J Anat. 1994; 184(Pt 3):477–492. [PubMed: 7928637]
48. Regatte RR, Akella SV, Borthakur A, et al. Proteoglycan depletion-induced changes in transverse relaxation maps of cartilage: comparison of T2 and T1rho. Acad Radiol. 2002; 9:1388–1394. [PubMed: 12553350]

49. Wheaton AJ, Dodge GR, Elliott DM, et al. Quantification of cartilage biomechanical and biochemical properties via T1rho magnetic resonance imaging. Magn Reson Med. 2005; 54:1087–1093. [PubMed: 16200568]
50. Akella SV, Regatte RR, Wheaton AJ, et al. Reduction of residual dipolar interaction in cartilage by spin-lock technique. Magn Reson Med. 2004; 52:1103–1109. [PubMed: 15508163]
51. Nissi, MJ.; Mangia, S.; Michaeli, S., et al. Proc Intl Soc Magn Reson Med. Salt Lake City, UT, USA: 2013. Orientation anisotropy of rotating frame and T2 relaxation parameters in articular cartilage; p. 3552
52. Li X, Pai A, Blumenkrantz G, et al. Spatial distribution and relationship of T1rho and T2 relaxation times in knee cartilage with osteoarthritis. Magn Reson Med. 2009; 61:1310–1318. [PubMed: 19319904]
53. Xia Y, Moody JB, Alhadlaq H, et al. Imaging the physical and morphological properties of a multi-zone young articular cartilage at microscopic resolution. J Magn Reson Imaging. 2003; 17:365–374. [PubMed: 12594728]
54. Toth F, Nissi MJ, Wang L, et al. Surgical induction, histological evaluation, and MRI identification of cartilage necrosis in the distal femur in goats to model early lesions of osteochondrosis. Osteoarthritis Cartilage. 2015; 23:300–307. [PubMed: 25463443]
55. Lin PC, Reiter DA, Spencer RG. Classification of degraded cartilage through multiparametric MRI analysis. J Magn Reson. 2009; 201:61–71. [PubMed: 19762258]
56. Lukas VA, Fishbein KW, Reiter DA, et al. Sensitivity and specificity of univariate MRI analysis of experimentally degraded cartilage under clinical imaging conditions. J Magn Reson Imaging. 2014
57. Toffanin R, Mlynárik V, Russo S, et al. Proteoglycan depletion and magnetic resonance parameters of articular cartilage. Arch Biochem Biophys. 2001; 390:235–242. [PubMed: 11396926]
58. Julkunen P, Korhonen RK, Nissi MJ, et al. Mechanical characterization of articular cartilage by combining magnetic resonance imaging and finite-element analysis: a potential functional imaging technique. Phys Med Biol. 2008; 53:2425–2438. [PubMed: 18421123]
59. Zheng S, Xia Y. Effect of phosphate electrolyte buffer on the dynamics of water in tendon and cartilage. NMR Biomed. 2009; 22:158–164. [PubMed: 18720450]
60. Kahn D, Les C, Xia Y. Effects of cryopreservation on the depth-dependent elastic modulus in articular cartilage and implications for osteochondral grafting. J Biomech Eng. 2015; 137:054502. [PubMed: 25412272]
61. Zheng S, Xia Y, Bidthanapally A, et al. Damages to the extracellular matrix in articular cartilage due to cryopreservation by microscopic magnetic resonance imaging and biochemistry. Magn Reson Imaging. 2009; 27:648–655. [PubMed: 19106023]
62. Wang N, Xia Y. Dependencies of multi-component T2 and T1rho relaxation on the anisotropy of collagen fibrils in bovine nasal cartilage. J Magn Reson. 2011; 212:124–132. [PubMed: 21788148]
63. Wang N, Xia Y. Orientational dependent sensitivities of T2 and T1rho towards trypsin degradation and Gd-DTPA2- presence in bovine nasal cartilage. MAGMA. 2012; 25:297–304. [PubMed: 22071581]
64. Gröhn OH, Mäkelä HI, Lukkarinen JA, et al. On- and off-resonance T(1rho) MRI in acute cerebral ischemia of the rat. Magn Reson Med. 2003; 49:172–176. [PubMed: 12509834]

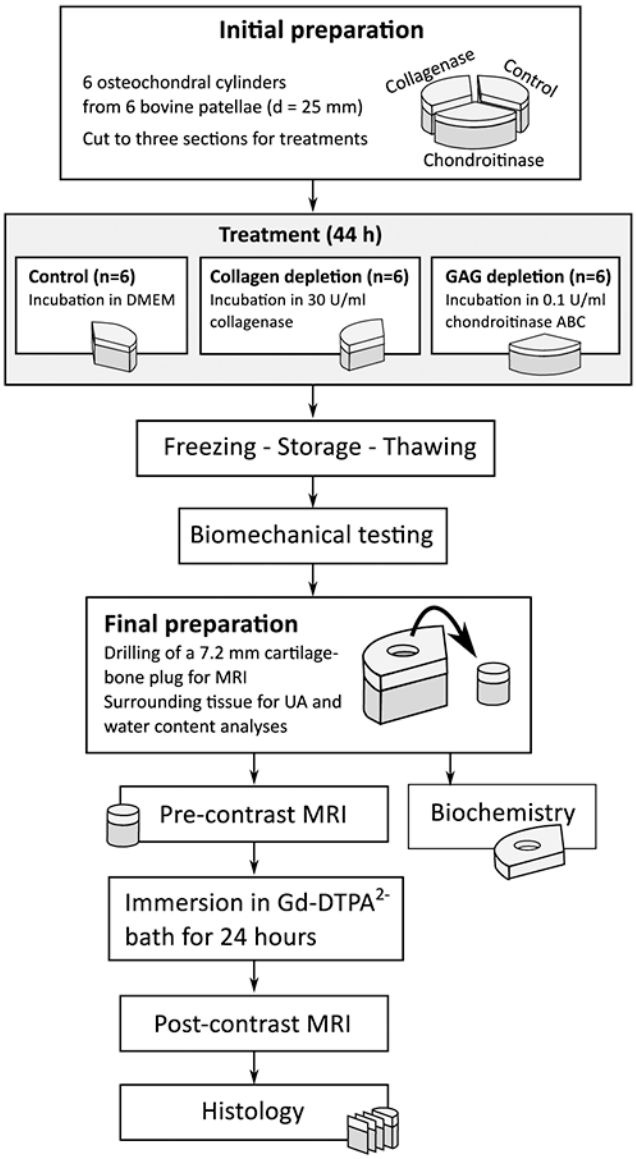

Figure 1.
Schematic presentation of the sample processing.

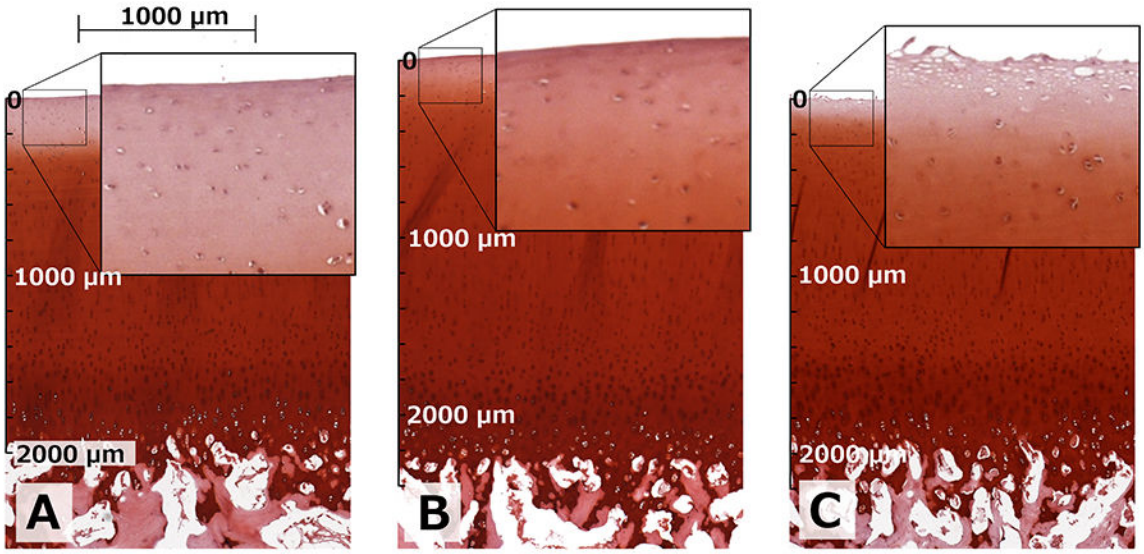

Figure 2.

Safranin-O-stained sections of different treatments from a representative specimen. Chondroitinase ABC-treated specimen (A), control specimen (B) and collagenase-treated specimen (C) from the same bovine patella. Zoom-ups visually depict the changes induced by the treatments in the adjacent tissue samples; reduced staining for GAGs was evident in the chondroitinase ABC-treated specimens whereas a destruction of the most superficial tissue was seen in the collagenase-treated specimens. Scale bars give comparable dimensions for each section starting from the articular surface.

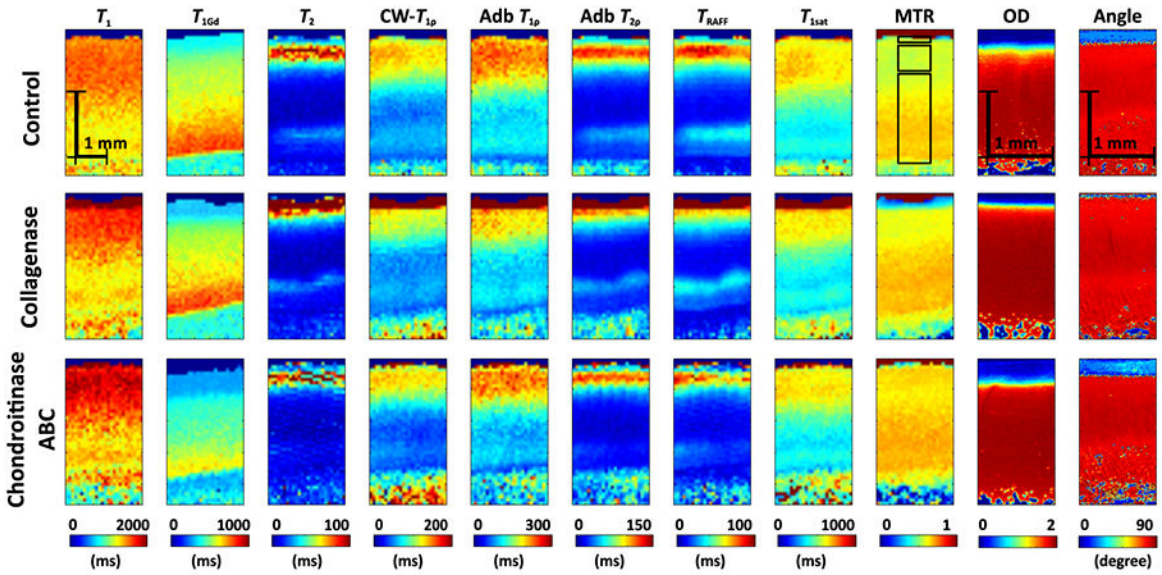

Figure 3.

Representative relaxation time maps for a specimen after control, collagenase and chondroitinase ABC treatments together with optical density and orientation angle maps as derived by digital densitometry and polarized light microscopy, respectively. Definition of the superficial, transitional and radial ROIs, in order starting from the top of the figure are exemplified on top of the control MTR map.

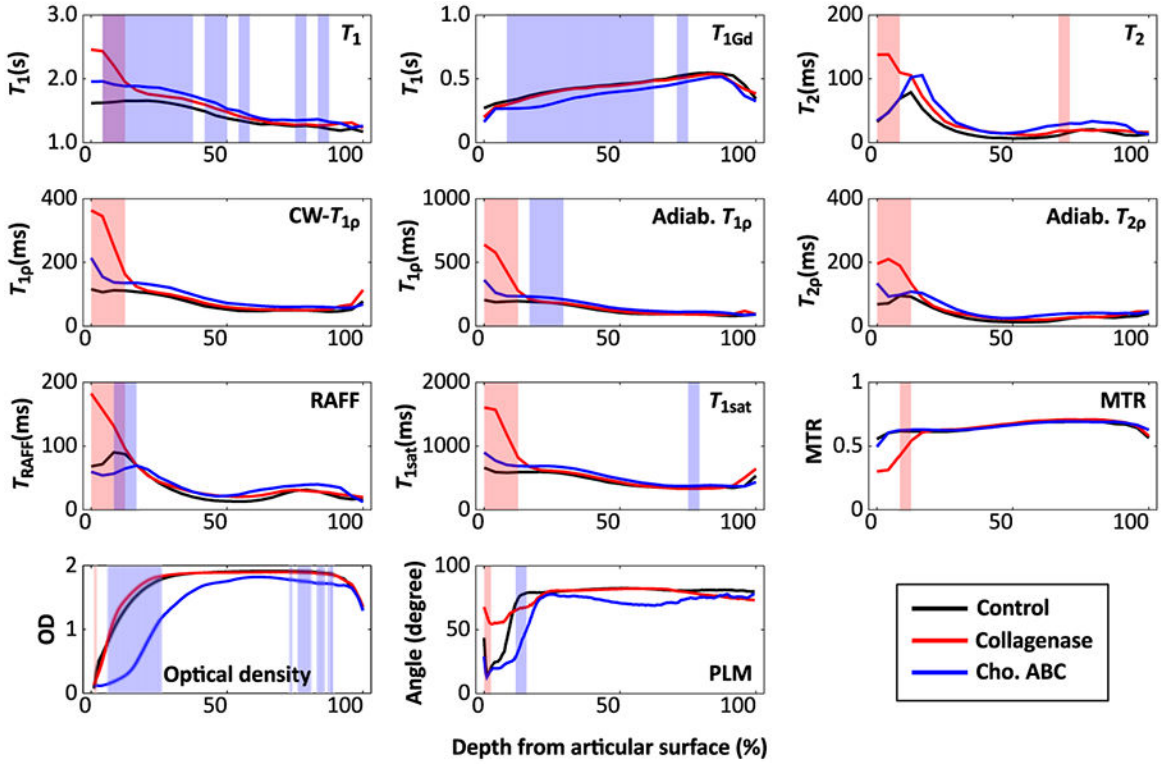

Figure 4.

Mean profiles along cartilage depth for MRI parameters, optical density and collagen orientation angle for the different sample groups. Shading indicates statistically significant ($p < 0.05$, Wilcoxon signed ranks test) differences between control and collagenase-treated (red), control and chondroitinase ABC-treated (blue), and control and both treatment groups (purple).

Table 1

Details of the preparation block elements. AHP = adiabatic half-passage pulse, AFP = adiabatic full-passage pulse (HS1), CW = continuous wave, SL = spin-lock.

Param.	Preparation	Prep. parameter	Value of prep. parameter	Pulse power
T_1, T_{1Gd}	Change of TR in the readout sequence	TR	80, 160, 320, 640, 1280, 2560, 5120 ms	-
T_2	Spin echo preparation	TE	4, 8, 16, 32, 64, 128 ms	-
CW-$T_{1\rho}$	+AHP, CW SL pulse, -AHP[64]	SL pulse duration	0, 10, 20, 40, 80, 160 ms	γB_1 = 1 kHz
Adiab. $T_{1\rho}$	Train of AFPs[20]	# AFPs	[0, 4, 8, 12, 24] × 4.5 ms	$\gamma B_{1,max}$ = 2.5 kHz
Adiab. $T_{2\rho}$	+AHP, train of AFPs, -AHP[20]	# AFPs	[0, 4, 8, 12, 24] × 4.5 ms	$\gamma B_{1,max}$ = 2.5 kHz
T_{RAFF2}	RAFF2 pulse train[23; 27]	# RAFF2 pulses	[0, 2, 4, 6] × 9 ms	$\gamma B_{1,max}$ = 625 Hz
MTR, T_{1sat}	CW saturation at -100 kHz and +10 kHz offset from water frequency, both with and without preceding 180° pulse[24]	Saturation duration	0, 0.1, 0.2, 0.4, 0.8, 1.6, 3.5, 7 s	γB_1 = 250 Hz

Table 2

Mean and 95% confidence interval of equilibrium moduli (E_{eq}), water contents (H_2O), uronic acid (UA) contents, and optical densities for the sample groups. Data are presented for bulk cartilage volume. *P* values indicate statistically significant differences between the treatment and control groups (Wilcoxon signed ranks test).

	Control	Collagenase	Change	Chondroitinase ABC	Change
E_{eq} (MPa)	0.77 (0.49, 1.04)	0.40 (0.30, 0.51)	-47.4% $p = 0.031$	0.25 (0.08, 0.43)	-67.1% $p = 0.031$
H_2O (%)	77.29 (75.53, 79.04)	79.13 (77.29, 80.98)	+2.4% $p = 0.156$	78.50 (77.07, 79.93)	+1.6% $p = 0.156$
UA (μg/mg/wet weight)	11.97 (11.02, 12.91)	11.00 (9.03, 12.98)	-8.0% $p = 0.313$	7.89 (5.44, 10.34)	-34.1% $p = 0.031$
Optical density (a.u.)	1.70 (1.61, 1.79)	1.71 (1.64, 1.78)	+0.9% $p = 0.563$	1.37 (1.05, 1.69)	-19.4% $p = 0.031$

Table 3

Linear (Pearson) correlation coefficients *r* between reference techniques and MRI parameters in full-thickness ROI.

Parameter	Equilibrium modulus	Uronic acid content	Water content	Optical density
T_1	-0.600, p=0.008	-0.324, p=0.190	0.257, p=0.302	-0.272, p=0.274
T_{1Gd}	0.434, p=0.072	0.699, p=0.001	-0.052, p=0.838	0.753, p=0.000
T_2	-0.427, p=0.077	-0.104, p=0.682	0.411, p=0.090	-0.112, p=0.658
CW-$T_{1\rho}$	-0.624, p=0.006	-0.292, p=0.239	0.504, p=0.033	-0.385, p=0.115
Adiab. $T_{1\rho}$	-0.618, p=0.006	-0.253, p=0.311	0.603, p=0.008	-0.310, p=0.210
Adiab. $T_{2\rho}$	-0.573, p=0.013	-0.361, p=0.140	0.464, p=0.052	-0.382, p=0.117
T_{RAFF2}	-0.385, p=0.115	-0.070, p=0.782	0.346, p=0.160	-0.086, p=0.734
T_{1sat}	-0.637, p=0.004	-0.113, p=0.655	0.613, p=0.007	-0.197, p=0.433
MTR	0.072, p=0.777	0.095, p=0.708	0.257, p=0.303	0.053, p=0.833